


Application of aeromagnetic and vertical electrical sounding to investigate groundwater potential in Dutse and Environs, Jigawa State, Nigeria

Applicazione dell'aeromagnetometria e dei sondaggi elettrici verticali per indagare il potenziale delle acque sotterranee a Dutse e dintorni, nello Stato di Jigawa, in Nigeria

Terhemba Shadrach BEM^a , Muhammad M. MACHINA^a, Daniel YANKARI^{a,b}, Hassan HARUNA^a, Suleiman A. MADAKI^a, Khalid Yusuf HAZO^a, Faith O. ADUDU^a

^a Department of Physics, Federal University Dutse, Jigawa State, Nigeria, email  : bem.shadrach@fud.edu.ng

^b Department of Physics, Sa'adu Zungur University Bauchi, Bauchi State, Nigeria

ARTICLE INFO

Ricevuto/Received: 09 February 2025

Accettato/Accepted: 30 June 2025

Pubblicato online/Published online:

30 September 2025

Handling Editor:

Antonio Menghini

Citation:

Bem, S.T., Machina, M.M., Yankari, D., Haruna, H., Madaki, S.A., Hazo, K.Y., Adudu, F.O. (2025). Application of aeromagnetic and vertical electrical sounding to investigate groundwater potential in Dutse and Environs, Jigawa State, Nigeria.

Acque Sotteranee - Italian Journal of Groundwater, 14(3), 09 - 20

<https://doi.org/10.7343/as-2025-861>

Correspondence to:

Terhemba Shadrach Bem 

bem.shadrach@fud.edu.ng

Keywords:

aeromagnetic, groundwater, resistivity method, basement complex, Dutse.

Parole chiave:

aeromagnetometria, acqua sotterranea, metodo di resistività, complesso basale, Dutse.

Abstract

This study examines subsurface structures and their potential for groundwater exploration using integrated geophysical datasets, including Magnetic and Vertical Electrical Sounding (VES). In processing the magnetic data, various filters such as Upward Continuation (UC), First Vertical Derivative (FVD), analytic signal, and Source Parameter Imaging (SPI) were applied to enhance the structural attributes and estimate the depths of magnetic structures (basement). The residual and UC maps reveal a strong magnetic high in the northern and southern regions, potentially linked to lithological variations or an undulated basement. Specifically, we delineated a prominent NE-SW trending lineament interpreted as a geologic contact zone, which has never been identified in the area, serving as a pathway for groundwater flow. The depth to the basement is estimated to range from approximately 100 to 500 meters, with the deepest regions indicated around the Army barracks, the northeastern side, and Duste Town. The VES results indicate a deep aquifer in the Barracks and Northeastern axes, with a corresponding deep crystalline basement at depths that align with the SPI depth estimates. We identified a thick claystone and compact sandstone at the barracks and along the contact zone, which may be responsible for the low-yield boreholes. Overall, the deepest aquifer zone in the region lies between 70 and 100 meters. The study highlights key areas for promising groundwater exploration, with apparent resistivity (ρ_a) contrasts indicating potential aquifer accumulation. This information is essential for efficient groundwater exploration and future drilling attempts.

Riassunto

Questo lavoro è finalizzato allo studio delle strutture del sottosuolo e il loro potenziale per la ricerca di acque sotterranee, utilizzando set di dati geofisici integrati, tra cui la magnetometria ed i Sondaggi Elettrici Verticali (SEV). Nell'elaborazione dei dati magnetici, sono stati applicati vari filtri come la Upward Continuation (UC), la Derivata Prima Verticale (FVD), il segnale analitico e la Source Parameter Imaging (SPI) per migliorare gli attributi strutturali e stimare la profondità delle strutture magnetiche (basamento). Le mappe delle anomalie residue e della UC rivelano una elevata anomalia magnetica nelle regioni settentrionali e meridionali, potenzialmente legata a variazioni litologiche o alle ondulazioni del basamento. In particolare, abbiamo delineato un importante lineamento con direzione NE-SW, interpretato come una zona di contatto geologico, sino ad oggi non identificato nell'area, che funge da percorso per il flusso delle acque sotterranee. La profondità del basamento è stimata tra i 100 e i 500 metri circa, con le regioni più profonde indicate intorno alla caserma dell'esercito, al lato nord-orientale e alla città di Duste. I risultati dei SEV indicano una falda acquifera profonda in prossimità delle caserme e lungo l'asse nord-orientale, con un corrispondente basamento cristallino a profondità che si allineano con le stime prodotte dallo SPI. Abbiamo rilevato una potente argillite e un'arenaria compatta in corrispondenza della caserma e lungo la zona di contatto, che potrebbe essere responsabile dei pozzi a bassa produttività. Nel complesso, la zona acquifera più profonda della regione si trova tra i 70 e i 100 metri. Lo studio evidenzia aree chiave per una promettente ricerca delle acque sotterranee, con contrasti di resistività apparente (ρ_a) che indicano un potenziale accumulo acquifero. Queste informazioni sono essenziali per un'efficiente ricerca delle acque sotterranee e per i futuri tentativi di perforazione.

Introduction

The freshwater resource is under severe pressure globally due to the alarming population growth, economic development, and environmental changes such as climate change, global warming, and others. These factors collectively intensify water scarcity and strain existing infrastructure, requiring sustainable management strategies and innovative technologies to address today's global water challenges. In Nigeria, most rural population supplies their domestic water from underground sources such as Wells and Boreholes. As such, groundwater accessibility, preservation, and conservation are of paramount importance (Obeta, 2018; Okareh & Priscilla, 2014). Unfortunately, poverty, operational challenges, and most importantly, the complex geology of the regions pose significant challenges in identifying productive aquifers, as traditional exploration methods are often insufficient for delineating subsurface structures. This complexity necessitates the use of advanced exploration techniques like integrated geophysical surveys and hydrogeological modeling to better understand the subsurface structure and locate potential water resources.

Dutse region falls within the basement complex with a complicated aquifer distribution network in the subsurface.

There are usually large variations in hydrogeological properties over short distances, resulting in preferential pathways for fluid flow and reservoirs for accumulation (Day-lewis et al., 2017). Aquifer distribution and yield are significantly impacted by geological factors, notably the presence of fractures, faults, and the degree of weathering (Bello et al., 2024; Bon et al., 2022), which offer secondary porosity in the absence of primary porosity that boosts the yield of boreholes. These factors, when accurately delineated, can serve as precursors for effective site selection for maximum groundwater extraction. At the time of writing this paper, over 5 abortive borehole attempts were recorded at the 26 Armored Battalion Army Barrack Headquarters under construction in Duste, Jigawa state alone (Fig. 1). This was due to a lack of comprehensive information on the hydrology and geology of the region, resulting in huge financial losses. The urgent need to provide comprehensive data on the hydrology and geology for possible site selection for multiple productive boreholes in the Barracks and other difficult parts, Duste Metropolis, forms the drive behind this research.

Traditionally, various researchers have used different methods in exploring the underground for water, either by directly obtaining information on the potential occurrence of

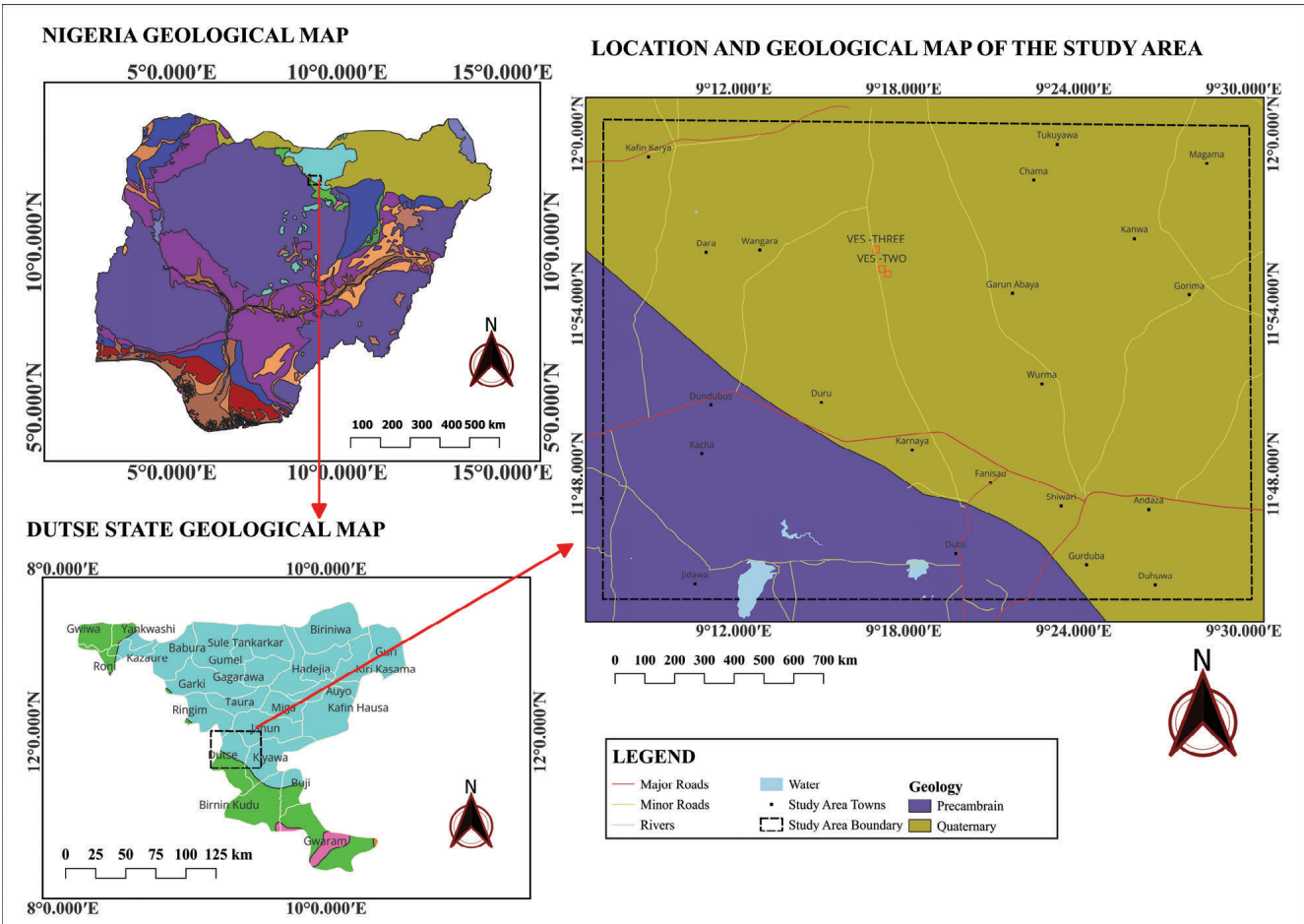


Fig. 1 - Location and Geological Map of the study area extracted from Nigeria and Jigawa State.

Fig. 1 - Ubicazione e Carta Geologica dell'area in studio, Jigawa State, Nigeria.

groundwater using techniques such as drilling, geophysical, geological, and hydrogeological (Ajayi & Adegoke-Anthony, 1988; Díaz-Alcaide & Martínez-Santos, 2019; Gomo & Ngobe, 2024; Ilugbo et al., 2023; Kim & Lekic, 2019; Sunkari et al., 2021; Ugbaja et al., 2021). The geophysics concept is the cheapest, and it has to do with the applications of laws of physics to provide information on groundwater potential and extraction (Okpoli & Akinbulejo, 2022). Different geophysical methods, such as magnetic (e.g., Hasan & Shang, 2021; Ndikilar et al., 2019), resistivity methods (e.g., Oyeyemi et al., 2022; Sawayama et al., 2023; Vogelgesang et al., 2019; Wu et al., 2023), and gravity (Epuh et al., 2020) have been used for groundwater exploration. These methods can be used as stand-alone or integrated for effective results. In particular, the magnetic method of geophysical prospecting is vital in investigating subsurface geology and identifying anomalous structures such as lineaments and basement topography resulting from the magnetic properties of the underlying rocks. Several studies delineated basement structural patterns and topography using aeromagnetic data (Emujakporue et al., 2018; Osinowo et al., 2014; Osinowo & Abdulmumin, 2019). Information about subsurface geometry, depth, thickness, and lateral extent of the impermeable crystalline basement is very crucial for accurate hydrogeological characterization of a given formation (Epuh et al., 2020; Ndikilar et al., 2019; Shevchenko & Iasky, 1997). The magnetic method integrated with electrical resistivity can harmoniously locate the permeable layers, fractures, and estimate their thicknesses, thereby providing a possible relationship between aquifers and related features (Awad et al., 2015).

In this research, the complementary advantages of magnetic and resistivity methods are leveraged to determine underground water potential zones in a highly problematic site in Duste, Nigeria. The study region covers the 26 Armored Battalion Army Barrack Headquarters, Dutse, Jigawa State, and its surrounding areas. The geology is characterized primarily by the Precambrian basement complex (Fig. 1), which consists of granitic and metamorphic rocks, with notable occurrences of schists and gneisses (Bala et al., 2011; Ndikilar et al., 2019; Obaje, 2009), particularly around Duste Metropolis. The area also features a weathered layer that varies in thickness and composition, significantly influencing groundwater recharge and availability. The northern part falls within the Quaternary formation, which generally consists of low-lying monotonous undulating sand dunes of various sizes, typical of the sedimentary Chad formation (Hassan et al., 2017). In Duste Town, outcropped rhyolite/ignimbrites with intensive jointing all over the exposure at the Turaki Tower and other places are visible on the surface. Rhyolite/ignimbrite rock, being an extrusive igneous rock with a high silica content, often has limited porosity and permeability, which can make the development of underground water sources more challenging than in typical granitic formation. Groundwater may be primarily found in fractures or faults rather than in large aquifers. Generally, the structural geology is marked by fractures and contact zones that provide

pathways for groundwater movement, making it essential to understand these features for effective groundwater management. The findings from this research are expected to provide critical insights into the sustainable management of groundwater resources in the area and contribute to the growing body of knowledge on hydrogeological investigations in Northern Nigeria.

Materials and Methods

Aeromagnetic Data and Processing

The aeromagnetic data used in this study were obtained from the Nigerian Geological Survey Agency (NGSA). The data was acquired by flying at a nominal altitude of 80 meters along north-south flight lines spaced 500 meters apart, ensuring higher resolution. The acquisition was between 2005 and 2009; hence, the geomagnetic gradient was corrected using the IGRF 2005 model, a standard method for accounting for the Earth's magnetic field variations. The UTM coordinate system, combined with the WGS 84 datum, was used for spatial referencing. The processed data were presented as Total Magnetic Intensity (TMI) maps. Figure 2 presents the TMI map of the study area, highlighting the intensity variations and wavelengths of local anomalies. These anomalies offer valuable insights into subsurface structures, which can be used to infer the geometry, depth, and boundaries of potential water-bearing formations, aiding in groundwater exploration. Regions such as the Army Barracks, Chamo, Dusti, and Jidawa fall within higher TMI values, typically indicating the presence of magnetic minerals and features such as igneous intrusions. Conversely, lower TMI values observed around Magama and Abaya, trending NE-SW, may correspond to sedimentary basins or contact zones where significant alteration has occurred.

The TMI data was first reduced to Equator (RTE) to remove asymmetries in anomalies associated with low magnetic latitude regions (Fantah et al., 2022; Oni et al., 2020). To generate the RTE, Geosoft extensions were utilized through the MAGMAP 1-step filtering option in Oasis Montaj. This involved selecting the appropriate filter settings in the Magmap Filter Design dialog box, inputting the survey data, and calculating the necessary fields for reduction to the equator. The regional and residual separation filter was then applied to extract the residual magnetic field, also known as the crustal field.

The application of Upward Continuation (UPC) is essential for delineating potential aquifer zones, as it enhances the identification of deeper geological structures while effectively reducing near-surface noise. This technique is particularly important in groundwater studies, where understanding subsurface conditions is critical for identifying viable aquifer formations. For groundwater investigations, a depth range of 500m to 1000m (1km) is suitable for distinguishing deeper anomalies that may indicate significant water-bearing zones (Salem & Ali, 2016). Care is, however, taken not to over-smooth the data, thereby removing shallow anomalies that could contribute to shallow aquifer zones. UPC is applied

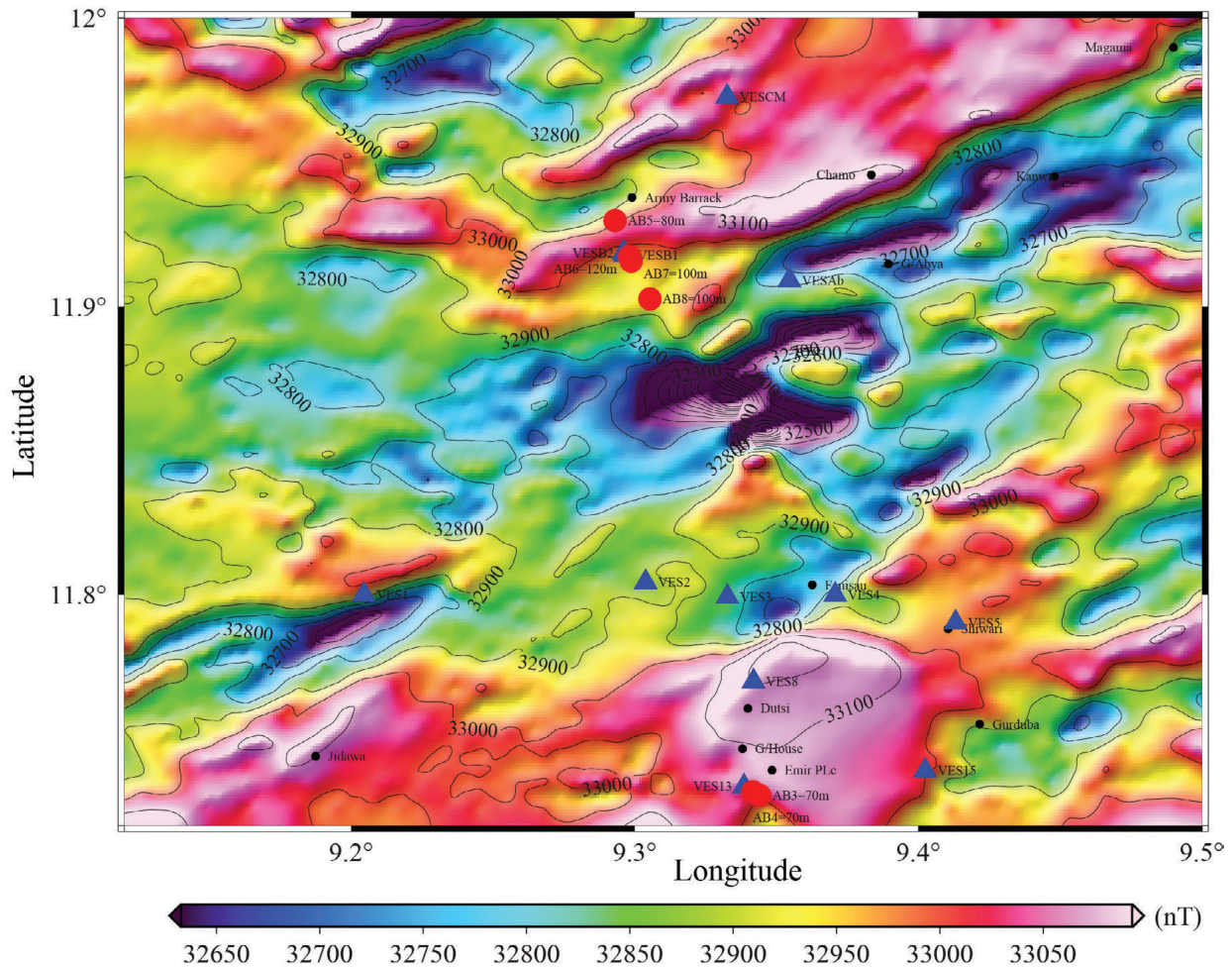


Fig. 2 - Total Field Aeromagnetic Map (TMI) of the study Area. The anomalies vary from 32633- 33100nT as shown by the color bar. Triangles are VES stations and the red circles, some of the abortive boreholes recorded in the regions.

Fig. 2 - Carta del Campo Magnetico Totale (TMI) dell'area in studio. Le anomalie variano da 32633 a 33100nT come mostrato dalla scala di colore. I triangoli indicano le stazioni SEV ed i cerchi rossi alcune perforazioni sterili registrate nelle regioni.

to the Reduced-to-Equator (RTE) data prior to computing different litho-structural magnetic analytic techniques, e.g., first vertical derivatives, Lineament maps, and depth to magnetic sources estimation technique using an appropriate menu of the Oasis Montaj (Fig. 3). The results retain the major magnetic anomalies and trends as observed on the residual map (Fig. 3). The major trends are in an NE-NW trending direction,

separated into a high magnetic anomaly in the north and south, with a low magnetic anomaly in the middle of the study region.

Another useful operation is the first vertical derivative (FVD) applied to potential field data to enhance the effects of shallow features that could easily be overshadowed by regional anomalies (Fantah et al., 2022; Salem et al., 2014). It is more responsive to local influences than to regional effects by highlighting high-frequency features (Fantah et al., 2022). We calculated the FVD using the UC map in the frequency domain, with respect to the x, y, and z axes, and their derivatives dx, dy, and dz. The FVD data were instrumental in producing the lineament (Fig. 3d), which is critical for

identifying structural trends. The sequence of processing was in the following order: TMI→RTE→Residual→UPC→FVD and other analyses such as analytic signal and source parameter imaging. The analytic signal technique is based on the use of the first derivative of magnetic anomalies to estimate source characteristics and to locate positions of geologic boundaries such as contacts and faults. The amplitude of the Analytic Signal is defined as the square root of the squared sum of the vertical and the two horizontal first derivatives of the magnetic field anomaly T and is given by (Li & Nabighian, 2015):

$$A(x, y) = \sqrt{\left(\frac{\partial T}{\partial x}\right)^2 + \left(\frac{\partial T}{\partial y}\right)^2 + \left(\frac{\partial T}{\partial z}\right)^2} \quad (1)$$

Where,

A(x,y) is the analytic signal, $\left(\frac{\partial T}{\partial x}\right)$, $\left(\frac{\partial T}{\partial y}\right)$, $\left(\frac{\partial T}{\partial z}\right)$ are the partial derivatives of the total magnetic intensity (T) with respect to the horizontal and vertical coordinates (x, y, z). The analytic signal allows the identification of anomalies without being affected by the direction of the magnetic field, and magnetic

remanence, and thus relates directly with the local geology (Osinowo et al., 2023), making it particularly useful for estimating the depth and geometry of subsurface structures, which is essential in groundwater exploration.

The depth of the crystalline basement is crucial for delineating potential underground water zones in a basement complex. In particular, the basement's depth influences the extent and characteristics of overlying weathered zones and fracture networks, which act as conduits and reservoirs for groundwater. Understanding the basement's topography helps in predicting the spatial distribution of these water-bearing features, thus aiding in water resource exploration and management. The Source Parameter Imaging (SPI) was employed to assess the basement depth, aiding in identifying potential groundwater-bearing formations. It is a semi-automatic method for estimating the depths of magnetic sources (Thurston & Smith, 1997). Based on the complex analytic signal, SPI calculates source parameters from gridded magnetic data, assuming a 2D sloping contact or a 2D dipping thin-sheet model (Li & Nabighian, 2015; Thurston & Smith, 1997). Using Oasis Montaj, the depths were determined by applying first vertical derivatives and horizontal gradients to the magnetic data (Thurston & Smith, 1997). This method simplifies the interpretation process, providing accurate depth estimates for each anomaly, which are then visualized on a map to better identify groundwater potential zones. The depth (Z) to the magnetic source is typically calculated using Equation 2.

$$Z = \frac{1}{\left(\left[\frac{dA}{dx} \right]^2 + \left[\frac{dA}{dy} \right]^2 \right)_{\max}} \quad (2)$$

Where:

Z = Depth of the magnetic source; A = tilt derivative;

$k = \left(\left[\frac{dA}{dx} \right]^2 + \left[\frac{dA}{dy} \right]^2 \right)$, is the local wavenumber over the

step-source. SPI algorithm computes for A and K then it finds maximum values (Meneisy et al., 2021; Thurston & Smith, 1997).

Vertical Electrical Sounding

Vertical Electrical Sounding (VES) is a resistivity method commonly used in groundwater exploration to measure ground resistance variations with depth (Yelwa et al., 2015). It involves injecting current into the ground through a set of electrodes at different spacings, and the potential difference is measured with another set of electrodes, from which the apparent resistivity ($\rho\alpha$) values can be calculated (Loke et al., 2013). VES has several limitations when used as a standalone method in underground water investigation. Due to the large variation in subsurface resistivity and the inherent non-uniqueness of inversion models, the method sometimes leads to misinterpretation of the layers' parameters (M. Metwaly,

2012). It is therefore necessary to interpret the sounding data using prior information from other geophysical results and geological data. This underpins an integrated approach using magnetic and/or gravity data along with VES (M. Metwaly, 2012; Ndikilar et al., 2019; Vogelgesang et al., 2019; Yelwa et al., 2015). In a typical basement complex, having prior knowledge of the structural network of lineaments identified from magnetic data interpretation and the depth to the top of the basement can significantly improve the accuracy of VES model interpretations.

We used the ABEM SAS 1000 Terrameter to collect subsurface resistivity data to complement the results of the aeromagnetic data interpretation (López Loera et al., 2015; Ndikilar et al., 2019). The surveying locations were randomly selected within the zones of high lineament clustering (Fig. 3). Several VES points were surveyed, and the apparent resistivity ($\rho\alpha$) values were calculated using the formula:

$$\rho\alpha = k \cdot R \quad (3)$$

Where k is the geometric factor for the Schlumberger array configuration employed in this study, and R is the measured resistance.

$$k = 2\pi \left\{ \left(\frac{1}{r_1} - \frac{1}{r_2} \right) - \left(\frac{1}{r_3} - \frac{1}{r_4} \right) \right\}^{-1} \quad (4)$$

r_n (n = 1, 2, 3, 4) Is the inter-electrode spacing. The $\rho\alpha$ data were qualitatively and quantitatively interpreted using a modeling technique to estimate the $\rho\alpha$ distribution and layer parameters such as layer thicknesses and the overall geological structure (Sunkari et al., 2021).

Results and Discussion

Magnetic data interpretation

The Residual map displays magnetic intensity ranging from about -200 nT to 100 nT (Fig. 3a). A strong positive magnetic anomaly trending in an NE-SW direction is observed on the Northeastern side covering Magama, Chamo, and on the southern side of the region in Duste Town and Jidawa. This corresponds to the elevated granitic mountains located in Duste, Emir Palace, and other areas of the study area that may be covered by deposited Chad formation materials. These anomalies have a deep origin, as observed in the results of the upward continuation to a depth of 500m (Fig. 3b). The smoothed anomaly map revealed an enhanced magnetic low trending in NE-SW between the Northeastern magnetic high and the southeastern magnetic high. This strong magnetic variation may indicate a variation in the subsurface geology and discontinuities in the basement rock (caused by faulting, fracturing, or jointing). It could also suggest an undulated basement relief or the degree of alteration (Oni et al., 2020).

To delineate the direction of the underground water flow path, the trend analysis is important (Meneisy et al., 2021). The FVD (Fig. 3c) gives the changes in the magnetic field with respect to depth, highlighting anomalous variations in

magnetic susceptibility. The FVD map reveals structural trends that can be interpreted as geological features such as faults, ore bodies, basin edges, or simply lineaments. We extracted the lineaments from the FVD data (Fig. 3d). These lineaments are indicative of structural elements such as faults, fractures, and geological contacts that can influence the movement of groundwater (Lee et al., 2012; Meneisy et al., 2021). We have grouped the lineaments into four groups (A, B, C, and D). We observed that B and C are likely originating from the same geologic structure inferred to be a contact zone with a NE-SW orientation. Lee et al (2012) described a geologic lineament as a linear zone of weakness in the Earth's crust that may owe its origin to tectonic or glacial causes and often represents geologic features such as faults, dykes, lithologic contacts, and structural form lines. Since no previous studies have mapped a fault zone in our study region, it is safe to call the trend in our magnetic interpretation a geologic lineament.

Generally, the dominant structures comprising the geologic lineament exhibit an NE-SW trending orientation that aligns with the trend of the main magnetic anomalies, as highlighted in the residual and upward continuation maps. The northern part (Chamo, Magama, and the Army Barracks) falls within the Quaternary formation, which primarily consists of low-lying, monotonous, undulating sand dunes characterized by sandstones and claystone, typical of the sedimentary Chad formation (Hassan et al., 2017). The contact zone between the northern sedimentary and the southern magmatic mountains constitutes the primary subsurface structure influencing groundwater flow and potential borehole yield in the region. Secondary trends, such as NW-SE and N-S, while less significant in our study area, may still contribute to localized water movement. One important application of this information is in determining the direction and location of geophysical field observations for groundwater and mineral exploration. Geophysical profiling, such as resistivity and

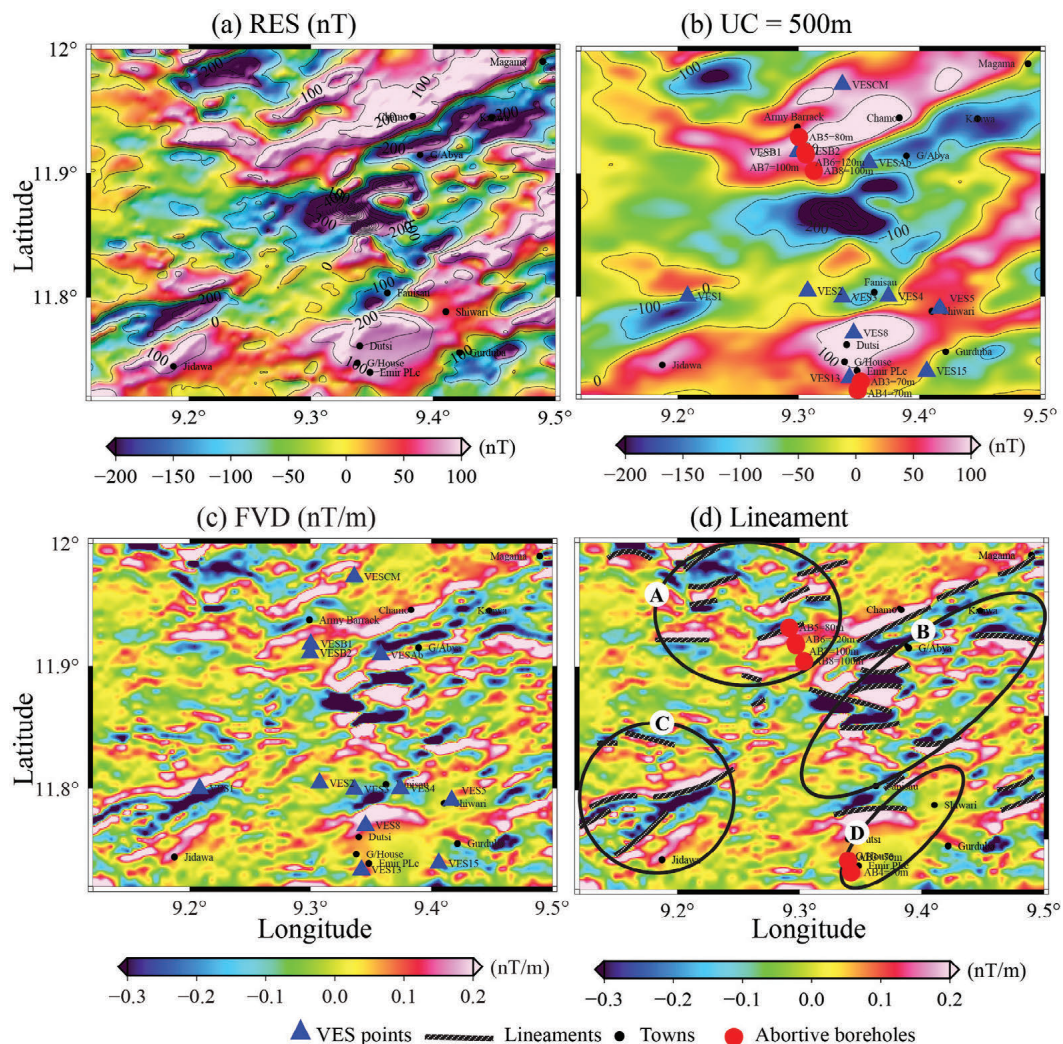


Fig. 3 - Results of aeromagnetic data processed with different filters (a) residual separation, (b) Upward continuation at 500m, (c) First vertical derivative, and (d) the lineament map (zebra lines) overlaid on the FVD. The circled regions A, B, C, and D are the interpreted zones of dense lineament clusters suitable for underground water development.

Fig. 3 - Risultati dell'elaborazione dei dati magnetici, tramite filtri differenti (a) separazione delle anomalie residue, (b) Upward continuation a 500m, (c) Derivata Prima Verticale (FVD) e (d) mappa di lineamenti (linee zebra) sovrapposte al FVD. Le regioni cerchiata A, B, C e D rappresentano le zone interpretate come a maggior densità di lineamenti, idonee alla costituzione di risorse idriche sotterranee.

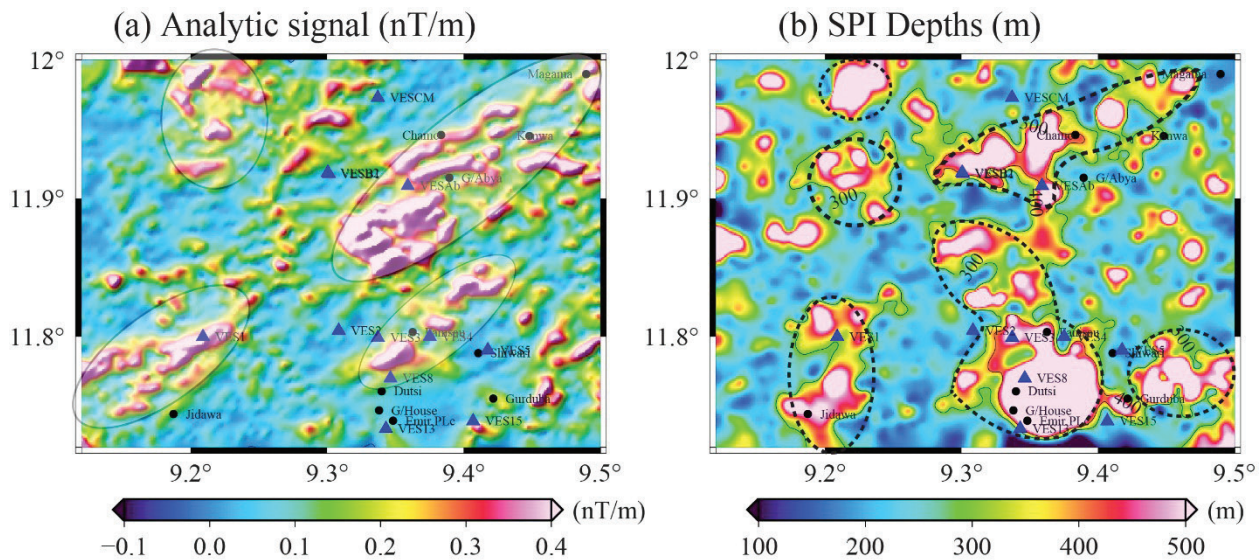


Fig. 4 - The Analytical map showing the main regional trends (a) and the Source Parameter Imaging (SPI) depth map of the Study Area (b). Zones of deep basement depth/thick sedimentary cover are enclosed in the dotted lines.

Fig. 4 - La Mappa Analitica mostra i principali trends regionali (a) e la carta di profondità del Source Parameter Imaging (SPI) dell'area in studio (b). Le zone di elevata profondità del basamento/potente copertura sedimentaria sono racchiuse nelle linee punteggiate.

seismic, will reveal significant anomalies when performed in an NN-SS or NW-SE direction, intersecting the major geologic lineament, rather than when performed parallel to the trend. Therefore, drilling along the NE-SW axis is recommended for optimal groundwater exploration, while the secondary trends may provide supplementary pathways for groundwater. We also analyzed the analytic signal map (Fig. 4a), This highlights strong and distinct NE- SW trending magnetic signatures that divide the area diagonally into two halves, with magnetic intensity ranging from -0.1 to 0.4 nT/m, potentially indicating groundwater- bearing features interpreted as a contact zone. In contrast, medium to low analytic signal amplitudes are observed across the NW, SE, and parts of the NE, which may correspond to areas with less pronounced geological features. The spatial variation in signal amplitude offers key insights into subsurface heterogeneity, aiding in more accurate delineation of potential groundwater reservoirs and geological contacts.

The depth of the magnetic sources is important in interpreting structures for underground water potentials. The SPI depth estimates (Fig. 4b) reveal depths that range from 100 to 500m. This depth can be interpreted to be the depth to the crystalline basement, which forms the bottom of the Duste aquifer, and it is observed to be generally shallow (<300m) in most parts of the study area, except for a few scattered locations, notably Duste, Jidawa, Barracks, and Chamo. Generally, the basement depth is not deep except for locations where the Chad formation cuts into the area, offering a thick sediment and weathered zone. The variation in the depth distribution of basement rock highlights the complexity of the subsurface and provides valuable information for targeting areas with higher groundwater potential.

Vertical Electrical Sounding (VES)

Figure 5 illustrates the ρ_a data from most of the VES stations plotted on the same axis. All the curves demonstrate a gradual increase in ρ_a at shallow depths corresponding to the overburden material before decreasing at about 10-50 meters, indicating a transition from a more resistive, unsaturated layer to conductive, more saturated layers (including aquifer) with depth. At approximately 50-70 meters, the ρ_a increases steadily again, marking the transition from the weathered layer to the fractured and/or crystalline basement layer that may extend indefinitely. The survey results indicate the presence of an unconfined aquifer at most locations typical of basement formation, with an average thickness of 20 meters comprising the weathered and/or fractured zone, which is capable of supplying large quantities of groundwater.

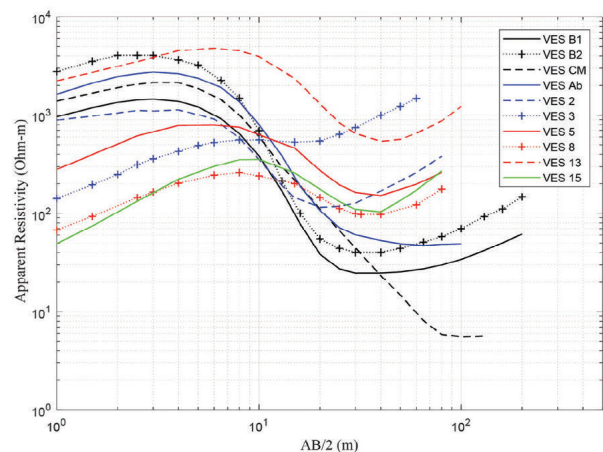


Fig. 5 - A plot of all apparent resistivity curves (Fig. 3c) on the same axis. Most of the curves have similar shapes, typically four-layered curves.

Fig. 5 - Un insieme di tutte le curve di resistività apparente (Fig. 3c). La maggior parte delle curve ha forma simile, tipicamente a 4 strati.

To quantify aquifer parameters, we processed the ρ_a data by inverting the field data to obtain the models at each sounding station. The raw VES data is slightly smoothed or detrended to remove outliers and then inverted to obtain ρ_a plots iteratively. This iterative process refines the data for accurate parameter quantification, as shown in Figure 6 and Table 1. Typically, the RMS error, which measures the misfit between the model and the data, is used to determine the adequacy of the inversion. In most cases, a four-layered model provides the best fit to the data and the most geologically reasonable models, supported by the drilling work and previous studies in the region (Hamza et al., 2016; Ndikilar et al., 2019). In VES B1 and B2 taken at the 26 Amoured Battalion Military Barracks, Duste, the ρ_a values increase gently from about 600-1800 Ωm in the first layer to ~ 2800 -10000 Ωm in the second layer ($\sim 2\text{m}$) before dropping drastically to 23-37 Ωm in the 3rd layers at the depths of ~ 50 -70 m. The fourth layers are characterized by high ρ_a values at infinite depth, interpreted to be fractured and crystalline basement. This is a typical KH-curve type defined by $\rho_{a1} < \rho_{a2} > \rho_{a3} < \rho_{a4}$ (Patra et al., 2016; Sunkari et al., 2021). The extremely low ρ_a of the 3rd layer indicates the presence of claystone. Several abortive boreholes have been drilled in the Barracks recently at depths of 80-100 m, revealing claystone and compact sandstone. The successful boreholes in the barracks extend to about ~ 120 -170 m depth with low to moderate yield. Generally, claystone and associated clayed formations have low

permeability, which limits their capacity to hold and transmit groundwater. Unless it is fractured or mixed with sand, boreholes drilled in a clayed formation are abortive or low-yield. The presence of claystone and compact sandstone at the barracks is the possible cause of abortive boreholes, especially when the depth is not reasonably deep enough.

VES CM and VES Ab were taken at the Chamo and Abaya settlements in the Northeast axis of the study region. This region coincides with the NE-SW trending magnetic high observed on the magnetic results, interpreted as a geologic contact zone. The VES curves are typical K-type curves defined by a low ρ_a topsoil layer that overlies a high-resistive layer interpreted to be consolidated lateritic stone, followed by a conductive layer at greater depths. The conductive layers are interpreted as the aquifer layers that correspond to the weathered and fractured basement. The thickness is beyond 100m, with the fresh basement not constrained in our VES measurement. However, the depth to the basement constrained in the magnetic results is about 500m. The Northeastern region possibly falls within the depositional part of Duste, where Chad formation is observed, similar to VES B1 and B2. Unpublished drilling report of boreholes at Chamo and Abaya reveals a very high yield, with the aquifer observed to be coarse sandstone and sandy clays (Table 1). VES CM and VES Ab were taken at the Chamo and Abaya settlements in the Northeast axis of the study region. This region coincides with the NE-SW trending magnetic high observed on the

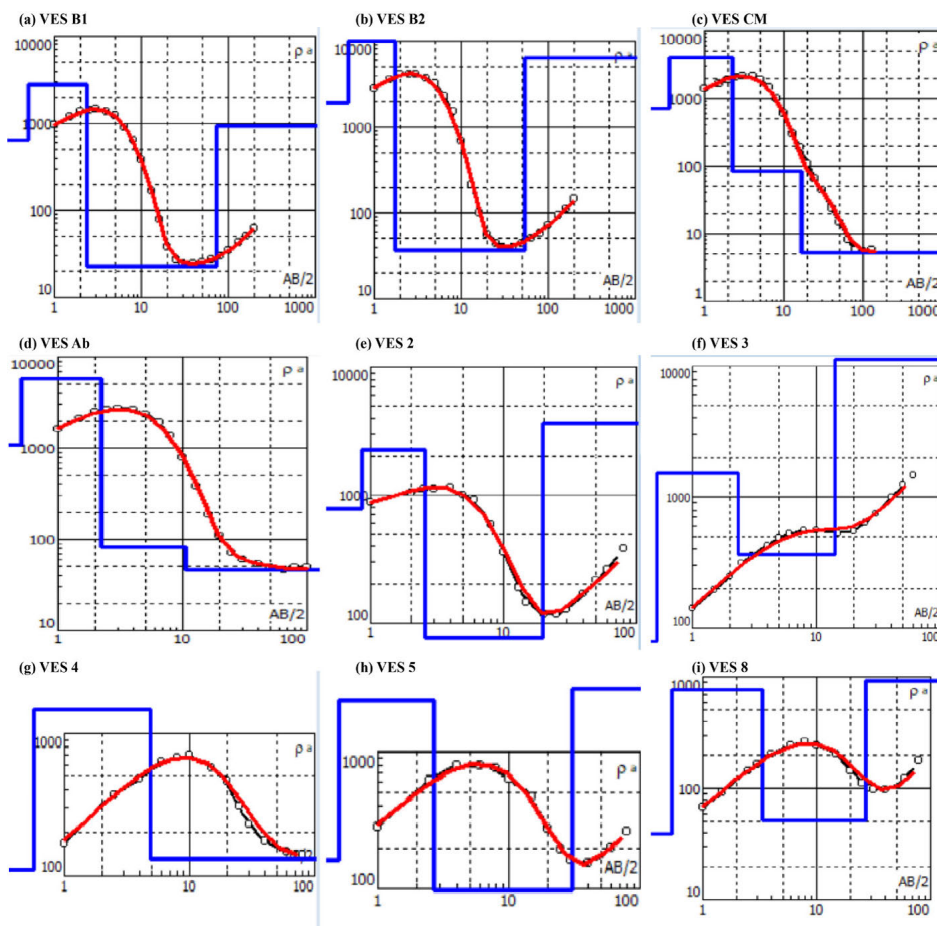


Fig. 6 - VES modeled results. The red and black curves are the synthetic and the data curves, respectively. The blue step-wise lines give the layered model defined for the synthetic and fitted to the data.

Fig. 6 - Modelli dei SEV. Le curve rosse e nere sono rispettivamente i sintetici ed i dati di campagna. I modelli riferiti ai dati sintetici che fittano i dati di campagna, sono rappresentati in blue.

magnetic results, interpreted as a geologic contact zone. The VES curves are typical K-type curves defined by a low ρ_a topsoil layer that overlies a high-resistive layer interpreted to be consolidated lateritic stone, followed by a conductive layer at greater depths. The conductive layers are interpreted as the aquifer layers that correspond to the weathered and fractured basement. The thickness is beyond 100m, with the fresh basement not constrained in our VES measurement. However, the depth to the basement constrained in the magnetic results

is about 500m. The Northeastern region possibly falls within the depositional part of Duste, where Chad formation is observed, similar to VES B1 and B2. Unpublished drilling report of boreholes at Chamo and Abaya reveals a very high yield, with the aquifer observed to be coarse sandstone and sandy clays (Table 1).

The rest of the sounding curves (VES 2, 3, 4, 5, and 8) fall around Duste Town. The characteristic curves are typically the KH-type. The top layer is made of low ρ_a , which is

Tab. 1 - VES model parameters, corresponding RMS (%) and the inferred lithology/description.

Tab. 1 - Parametri dei modelli SEV, RMS (%) corrispondente e descrizione delle litologie interpretate.

VES Points	Model parameters					Lithology/Description
	Number of Layers	ρ_a (Ωm)	Thickness (m)	Depth (m)	RMS (%)	
VES B1	1	638	0.5	0.5	0.20	Top soil
	2	2783	1.83	2.33		Laterite
	3	23.1	70.7	73		Sandy clay (Aquifer)
	4	936	∞	∞		Compact Sandstone
VES B2	1	1893	0.5	0.5	5	Top soil
	2	10000	1.25	1.75		Laterite
	3	37	52	53.7		Sandy clay (aquifer)
	4	6471	∞	∞		Compact Sandstone
VES CM	1	713	0.365	0.365	8	Top soil
	2	4008	1.89	2.25		Laterite sand
	3	83.9	14.4	16.6		Coarse sandstone (aquifer)
	4	5.3	∞	∞		Clay
VES Ab	1	1080	0.5	0.5	2.5	Top soil
	2	5775	1.69	2.19		Laterite sand
	3	81.2	8.53	10.7		Coarse sandstone (aquifer)
	4	47	∞	∞		Sandy Clay (aquifer)
VES 2	1	785	0.867	0.867	5.3	Top soil
	2	2234	1.68	2.55		Laterite sand
	3	76	17	19.6		Weathered basement
	4	3683	∞	∞		Granitic basement
VES 3	1	84	0.55	0.55	5.3	Top soil
	2	1788	2	2.56		Laterite sand
	3	182	6.14	8.7		Weathered basement
	4	9189	∞	∞		Granitic basement
VES 4	1	110	0.56	0.56	6.4	Top soil
	2	1476	4.31	4.89		Laterite sand
	3	131	∞	∞		Weathered basement
VES 5	1	163	0.5	0.5	3.3	Top soil
	2	2382	2.19	2.69		Laterite sand
	3	98	28.1	30.8		Weathered basement
	4	2905	∞	∞		Granitic basement
VES 8	1	40	0.56	0.56	5.6	Top soil
	2	768	2.8	3.36		Laterite sand
	3	54	22.7	26.2		Weathered basement
	4	912	∞	∞		Fractured basement

interpreted as sandy clay and depositional materials, with the second layer dry and unsaturated (Ndikilar et al., 2019). The average overburden thickness in Duste and its surroundings is between 0-15m (Hamza et al., 2016; Ndikilar et al., 2019) and comprises lateritic soil, sand, and sandy clay. The third layer with a relatively lower ρ_a value is interpreted to be the weathered basement, with ρ_a that ranges between 54-182 Ωm and aquifer depth between 20-30m. Below it is underlain by a high ρ_a material which could be interpreted as a low fissures basement complex (crystalline). Porous and permeable rock units, as well as the presence of thick weathered basement (regolith) and fractured rock formation, are the targeted formations for underground water development in the basement complex around Duste Town. Previous studies and drilling works reveal predominantly granitic rock with fractures at the depth of ~30m-75m, which constitute the main aquifer layers (Ndikilar et al., 2019). Fissures and interconnected fractures at this depth constitute conduits for groundwater occurrence, storage, and transmission. Generally, VES points with high ρ_a in the 3rd layer around Duste as observed in VES 3, may not be suitable for underground water development, since these areas may have a lower fracture network. In addition, some VES points may have shallow aquifer depth (VES 2, 3), generally about 20m.

Conclusions

This study combines magnetic and resistivity methods to offer a clearer picture of the subsurface geology and its potential for groundwater exploration. The magnetic maps reveal key structures, such as fractured zones and geologic contacts, particularly the NE-SW and NW-SE trending lineaments, indicating possible pathways for groundwater flow. The strong NE-SW trending magnetic anomaly in the study area may point contact zone that has yet to be identified, necessitating further investigation. Circular and elongated magnetic anomalies around Duste also suggest the presence of geological formations like intrusions, which are crucial for understanding how water moves and accumulates beneath the surface. The depth to the basement is estimated to range from 100 to 500 meters, with the deepest regions noted around the Army barracks, Chamo, the northeastern area, and Duste Town. The resistivity results from the VES surveys further validate these findings. In particular, the VES points collected at the Barracks, Chamo, and northeastern side indicate a deep aquifer that may extend beyond 100 meters, signifying a deeply seated crystalline basement. Anywhere else, the depth to the aquifer averages between 70 and 100 meters, suggesting that most boreholes would perform well between 70 and 100 meters, except in the Army barracks and along the NE-SW trending lineament, where the basement is deeply seated. Our integrated geophysical techniques help pinpoint areas where groundwater is most likely to be discovered. The low- ρ_a zones at greater depths present promising targets for drilling, especially along the NE-SW axis. Abortive boreholes are prevalent in the north due to the

presence of a thick claystone and compact sandstone identified using VES at the Barracks. Claystone and associated clay formations exhibit low permeability, limiting their ability to retain and transmit groundwater. Unless fractures exist in the basement that link to the weathered zone, boreholes drilled in the barracks shallower than 100m will likely be abortive or have low yields.

Competing interest

The authors declare no competing interest.

Acknowledgments

Our profound gratitude goes to Salem Geosolutions Limited for providing the technical support and making available their equipment for the resistivity data acquisition in this research. We also acknowledge the contributions of the postgraduate students of the Physics Department, Federal University Duste (Geophysics Group) during the data acquisition.

Finally, we wish to extend our gratitude to the anonymous reviewers for their constructive comments and suggestions that implementation have improved the quality of our manuscript.

Author contributions

Terhemba Shadrach Bem: Conceptualization, Funding acquisition, Resources, Supervision, Investigation, Visualization, Writing – original draft, and Editing. Muhammad M. Machina: Data acquisition, Processing, Writing – original & editing. Daniel Yankari: Data acquisition, Processing, Writing- review, and editing. Hassan Haruna: Data acquisition, Formal analysis, Writing – review & editing. Suleiman A. Madaki: Data acquisition, Formal analysis, Writing – review & editing. Khalid Yusuf Hazo: Formal analysis, Writing-review & editing. Adudu Faith: Data acquisition, Formal analysis, Writing – review & editing. All authors read and approved the final version of the manuscript.

Funding source

The authors received no external funding for this research.

Additional information

DOI: <https://doi.org/10.7343/as-2025-861>

Reprint and permission information are available writing to acquesotterranee@anipapozzi.it

Publisher's note Associazione Acque Sotterranee remains neutral with regard to jurisdictional claims in published maps and institutional affiliations.

REFERENCES

- Ajayi, O., & Adegoke-Anthony, C. W. (1988). Groundwater prospects in the Basement Complex rocks of southwestern Nigeria. *Journal of African Earth Sciences*, 7(1), 227–235.
- Awad, S., Araffa, S., Helaly, A. S., Khozium, A., Lala, A. M. S., Soliman, S. A., & Hassan, N. M. (2015). Delineating groundwater and subsurface structures by using 2D resistivity, gravity and 3D magnetic data interpretation around Cairo – Belbies Desert road, Egypt. *NRIAG Journal of Astronomy and Geophysics*, 4(1), 134–146. <https://doi.org/10.1016/j.nrjag.2015.06.004>
- Bala, A. E., Eduvie, O. M., & Byami, J. (2011). Borehole depth and regolith aquifer hydraulic characteristics of bedrock types in Kano area, Northern Nigeria. *African Journal of Environmental Science and Technology*, 5(3), 228–237. <https://doi.org/10.5897/AJEST10.194>
- Bello, Y., Abdulhakeem, A., & Yakubu, M. (2024). Assessing the challenges of viability of borehole through the extraction of lineaments from aeromagnetic data within a hostel at Air Force Institute of Technology, Kaduna, Nigeria. *Dutse Journal of Pure and Applied Sciences*, 10(2a), 150–160. <https://doi.org/10.4314/dujopas.v10i2a.14>
- Bon, A. F., Ombolo, A., Biboum, P. M., Moutlen, J. M., & Mboudou, G. E. (2022). Identification of hydrogeological features using remote sensing and electromagnetic methods in the hard- rock formations of the Cameroon coastal plain (Central Africa): implications for water borehole location. *Scientific African*, 17. <https://doi.org/10.1016/j.sciaf.2022.e01272>
- Day-lewis, F. D., Slater, L. D., Day-lewis FD, Slater LD, Robinson J, et al (2017) An overview of geophysical technologies appropriate for characterization and monitoring at fractured-rock sites. *J Environ Manage* 1–12. <https://doi.org/10.1016/j.jenvman.2017.04.033>
- Díaz-Alcaide, S., & Martínez-Santos, P. (2019). Review: Advances in groundwater potential mapping. *Hydrogeology Journal*, 27(7), 2307–2324. <https://doi.org/10.1007/s10040-019-02001-3>
- Emujakporue, G., Ofoha, C. C., & Kiani, I. (2018). Investigation into the basement morphology and tectonic lineament using aeromagnetic anomalies of Parts of Sokoto Basin, North Western, Nigeria. *Egyptian Journal of Petroleum*, 27(4), 671–681. <https://doi.org/10.1016/j.ejpe.2017.10.003>
- Epuh, E. E., Okolie, C. J., Daramola, O. E., Ogunlade, F. S., Oyatayo, F. J., Akinnusi, S. A., & Emmanuel, E. I. (2020). An integrated lineament extraction from satellite imagery and gravity anomaly maps for groundwater exploration in the Gongola basin. *Remote Sensing Applications: Society and Environment*, 100346. <https://doi.org/10.1016/j.rsase.2020.100346>
- Fantah, C., Armel, C., Fantah, C., Mezoue, C. A., Mouzong, M. P., Pierre, A., Kamga, T., Nouayou, R., & Nguia, S. (2022). Mapping of major tectonic lineaments across Cameroon using potential field data. *Earth, Planets and Space*. <https://doi.org/10.1186/s40623-022-01612-7>
- Gomo, M., & Ngobe, T. (2024). Groundwater exploration in a granite aquifer using the telluric electric frequency section method (TEFSM) in Eswatini, Southern Africa. *Sustainable Water Resources Management*, 10(1), 1–17. <https://doi.org/10.1007/s40899-023-01009-8>
- Hamza, S. M., Ahsan, A., Daura, H. A., Imteaz, M. A., Ghazali, A. H., & Mohammed, T. A. (2016). Fractured rock aquifer delineation and assessment using spatial analysis in Kano, Nigeria. *Arabian Journal of Geosciences*, 9(5). <https://doi.org/10.1007/s12517-016-2355-4>
- Hasan, M., & Shang, Y. (2021). Joint geophysical prospecting for groundwater exploration in weathered terrains of South Guangdong, China. *Environmental Monitoring and Assessment*. <https://doi.org/10.1007/s10661-021-09521-0>
- Hassan, H., Abdullahi, I. M., & Kwaya, M. Y. (2017). Groundwater chemistry, storage and dynamics in parts of Jigawa Central, Northwestern Nigeria. *Bayero Journal of Pure and Applied Science*, September. <https://doi.org/10.4314/bajopas.v10i1.19>
- Ilugbo, S. O., Aigbedion, I., & Ozezin, K. O. (2023). Structural mapping for groundwater occurrence using remote sensing and geophysical data in Ilesha Schist Belt, Southwestern Nigeria. In *Geology, Ecology, and Landscapes*. UBM Exhibition Singapore PTE LTD. <https://doi.org/10.1080/24749508.2023.2182063>
- Kim, D., & Lekic, V. (2019). Groundwater Variations From Autocorrelation and Receiver Functions. *Geophysical Research Letters*, 46(23), 13722–13729. <https://doi.org/10.1029/2019GL084719>
- Lee, M., Morris, W., Harris, J., & Leblanc, G. (2012). An automatic network-extraction algorithm applied to magnetic survey data for the identification and extraction of geologic lineaments. *The Leading Edge*, 31(1), 26–31. <https://doi.org/10.1190/1.3679324>
- Li, Y., & Nabighian, M. (2015). Tools and Techniques: Magnetic Methods of Exploration - Principles and Algorithms. In *Treatise on Geophysics: Second Edition* (Vol. 11, pp. 335–391). <https://doi.org/10.1016/B978-0-444-53802-4.00196-2>
- Loke, M. H., Chambers, J. E., Rucker, D. F., Kuras, O., & Wilkinson, P. B. (2013). Recent developments in the direct-current geoelectrical imaging method. *Journal of Applied Geophysics*, 95, 135–156. <https://doi.org/10.1016/j.jappgeo.2013.02.017>
- López Loera, H., Ramos Leal, J. A., Dávila Harris, P., Torres Gaytan, D. E., Martínez Ruiz, V. J., & Gogichaishvili, A. (2015). Geophysical Exploration of Fractured-Media Aquifers at the Mexican Mesa Central: Satellite City, San Luis Potosí, Mexico. *Surveys in Geophysics*, 36(1), 167–184. <https://doi.org/10.1007/s10712-014-9302-2>
- M. Metwaly. (2012). Groundwater exploration using geoelectrical resistivity technique at Al-Quwy'ya area Central Saudi Arabia. *International Journal of the Physical Sciences*, 7(2), 317–326. <https://doi.org/10.5897/IJPS11.1659>
- Meneisy, A. M., Al, M., Mohamed, D., & Deep, A. (2021). The Egyptian Journal of Remote Sensing and Space Sciences Investigation of groundwater potential using magnetic and satellite image data at Wadi El Amal , Aswan , Egypt q. *The Egyptian Journal of Remote Sensing and Space Sciences*, 24(2), 293–309. <https://doi.org/10.1016/j.ejrs.2020.06.006>
- Ndikilar, C. E., Idi, B. Y., Terhemba, B. S., Idowu, I. I., & Abdullahi, S. S. (2019). Applications of Aeromagnetic and Electrical Resistivity Data for Mapping Spatial Distribution of Groundwater Potentials of Dutse, Jigawa State, Nigeria. *Modern Applied Science*, 13(2), 11. <https://doi.org/10.5539/mas.v13n2p11>
- Obaje, N. G. (2009). The Basement Complex. In *Lecture Notes in Earth Sciences* (Vol. 120, pp. 13–30). https://doi.org/10.1007/978-3-540-92685-6_2
- Obeta, M. C. (2018). Rural water supply in Nigeria: Policy gaps and future directions. *Water Policy*, 20(3), 597–616. <https://doi.org/10.2166/wp.2018.129>
- Okareh, O. T., & Priscilla, A. I. (2014). Vertical Electrical Sounding and Groundwater Monitoring in a Tank Farm of Crude Oil Loading Terminal in Delta State, Nigeria. *International Research Journal of Geology and Mining*, 04(02), 64–76. <https://doi.org/10.14303/irjgm.2012.034>
- Okpoli, C. C., & Akinbulejo, B. Omobolanle. (2022). Aeromagnetic and electrical resistivity mapping for groundwater development around Ilesha schist belt, southwestern Nigeria. *Journal of Petroleum Exploration and Production Technology*, 12(3), 555–575. <https://doi.org/10.1007/s13202-021-01307-x>
- Oni, A. G., Eniola, P. J., Olorunfemi, M. O., Okunubi, M. O., & Osotuyi, G. A. (2020). The magnetic method as a tool in groundwater investigation in a basement complex terrain: Modomo Southwest Nigeria as a case study. *Applied Water Science*, 10(8), 1–18. <https://doi.org/10.1007/s13201-020-01279-z>
- Osinowo, O. O., & Abdulmumin, Y. (2019). Basement configuration and lineaments mapping from aeromagnetic data of Gongola arm of Upper Benue Trough, northeastern Nigeria. *Journal of African Earth Sciences*, 160(July), 103597. <https://doi.org/10.1016/j.jafrearsci.2019.103597>

- Osinowo, O. O., Abdulmumin, Y., & Victor, T. (2023). Energy Geoscience Analysis of high-resolution airborne-magnetic data for hydrocarbon generation and preservation potential evaluation of Yola sub-basins, northern Benue Trough, northeastern Nigeria. *Energy Geoscience*, 4(1), 33–41. <https://doi.org/10.1016/j.engeos.2022.08.002>
- Osinowo, O. O., Akanji, A. O., & Olayinka, A. I. (2014). Application of high resolution aeromagnetic data for basement topography mapping of Siluko and environs, southwestern Nigeria. *Journal of African Earth Sciences*, 99(PA2), 637–651. <https://doi.org/10.1016/j.jafrearsci.2013.11.005>
- Oyeyemi, K. D., Aizebeokhai, A. P., Metwaly, M., Omobulejo, O., Sanuade, O. A., & Okon, E. E. (2022). Assessing the suitable electrical resistivity arrays for characterization of basement aquifers using numerical modeling. *Heliyon*, 8(5), e09427. <https://doi.org/10.1016/j.heliyon.2022.e09427>
- Patra, H. P., Adhikari, S. K., & Kunar, S. (2016). *Groundwater Prospecting and Management*. Springer Singapore. <https://doi.org/10.1007/978-981-10-1148-1>
- Robinson, J., Johnson, C. D., Terry, N., & Werkema, D. (2017). An overview of geophysical technologies appropriate for characterization and monitoring at fractured-rock sites. *Journal of Environmental Management*, 1–12. <https://doi.org/10.1016/j.jenvman.2017.04.033>
- Salem, A., & Ali, M. Y. (2016). Mapping basement structures in the northwestern offshore of Abu Dhabi from high-resolution aeromagnetic data. *Geophysical Prospecting*, 64(3), 726–740. <https://doi.org/10.1111/1365-2478.12266>
- Salem, A., Green, C., Cheyney, S., Fairhead, J. D., Aboud, E., & Campbell, S. (2014). Mapping the depth to magnetic basement using inversion of pseudogravity: Application to the Bishop model and the Stord Basin, northern North Sea. *Interpretation*, 2(2), T69–T78. <https://doi.org/10.1190/INT-2013-0105.1>
- Sawayama, K., Ishibashi, T., Jiang, F., & Tsuji, T. (2023). Relationship Between Permeability and Resistivity of Sheared Rock Fractures : The Role of Tortuosity and Flow Path Percolation Geophysical Research Letters. 1–12. <https://doi.org/10.1029/2023GL104418>
- Shevchenko, S. I., & Iasky, R. P. (1997). Calculating depth to basement from magnetic and gravity data, with an example from the western Officer Basin. Geological Survey of Western Australia.
- Sunkari, E. D., Kore, B. M., & Abioui, M. (2021). Hydrogeophysical appraisal of groundwater potential in the fractured basement aquifer of the federal capital territory, Abuja, Nigeria. *Results in Geophysical Sciences*, 5(February), 100012. <https://doi.org/10.1016/j.ringps.2021.100012>
- Thurston, J. B., & Smith, R. S. (1997). Automatic conversion of magnetic data to depth, dip, and susceptibility contrast using the SPI (TM) method. *GEOPHYSICS*, 62(3), 807–813. <https://doi.org/10.1190/1.1444190>
- Ugbaja, A. A., William, G. A., & Ugbaja, U. A. (2021). Evaluation of groundwater potential using aquifer characteristics on parts of Boki Area, South- Eastern Nigeria. *Global Journal of Geological Sciences*, 19(1), 93–104. <https://doi.org/10.4314/gjgs.v19i1.8>
- Vogelgesang, J. A., Holt, N., Schilling, K. E., Gannon, M., & Tassier-surine, S. (2019). Using High-Resolution Electrical Resistivity to Estimate Hydraulic Conductivity and Improve Characterization of Alluvial Aquifers. *Journal of Hydrology*, 123992. <https://doi.org/10.1016/j.jhydrol.2019.123992>
- Wu, J., Dai, F., Liu, P., Huang, Z., & Meng, L. (2023). Application of the electrical resistivity tomography in groundwater detection on loess plateau. *Scientific Reports*, 13(1). <https://doi.org/10.1038/s41598-023-31952-7>
- Yelwa, N. A., Hamidu, H., Falalu, B. H., Kana, M. A., & I.M., M. (2015). Groundwater prospecting and Aquifer Delineation using Vertical Electrical Sounding (VES) method in the Basement complex terrain of Kumbotso Local Government Area of Kano State Nigeria. *IOSR Journal of Applied Geology and Geophysics (IOSR-JAGG)*, 3(1), 01–06. <https://doi.org/10.9790/0990-03110106>